Ocean Dynamics (2026) 76:25
https://doi.org/10.1007/s10236-026-01778-8

An operational real-time forecasting system for estuarine hydrodynamics: the Guadalquivir Estuary (SW Iberian Peninsula)

Pablo Muñoz-López[1,2] · **Simone Sammartino**[1,3] · **Jesús García-Lafuente**[1,2] · **Irene Nadal**[1,2] · **Antonio Bejarano**[4] · **Ángel Pulido**[4]

Received: 9 October 2025 / Accepted: 23 January 2026

Abstract

Accurate, real-time hydrodynamic forecasts are essential for understanding and managing short-term variability in estuarine systems. This study presents an operational real-time forecasting system for the Guadalquivir Estuary (SW Iberian Peninsula), a highly modified and regulated estuary of strong scientific and operational interest. The system is built on a three-dimensional Delft3D-Flow model that integrates, every 12-h, (i) astronomical and meteorological tide at the ocean boundary; (ii) regulated freshwater dam and tributary releases; and (iii) wind and surface heat-flux fields. Each operational cycle performs a 36-h hindcast followed by a 72-h forecast, completing the full 108-h integration in less than 25 min on a 24-core workstation. Validation against seven tide gauges during 2024 shows high predictable skill, with peak water level errors below 15 cm along the entire estuary and below 10 cm in the navigable reach, 6–10% of the tidal range, while Pearson correlations exceed 0.95. No systematic timing drift is detected between successive forecast cycles. Sensitivity tests show that the pragmatic treatment of unknown future forcings adds less than 4 cm to forecast error, well within the intrinsic model uncertainty. An automated alert protocol monitors forecast skill in near real time, supporting operational robustness. Overall, the system delivers reliable three-day water level predictions, demonstrating how numerical modeling, real-time validation, and uncertainty management can be combined to support operational oceanography in tidally dominated estuaries, with potential transferability to other estuarine systems worldwide.

Keywords Guadalquivir estuary · Operational oceanography · Hydrodynamic forecasting · Numerical modeling · Tidal dynamics · Real-time validation · Estuarine dynamics

Abbreviations

SAIH	Automatic database of hydrological information for river flood management
PdE	Puertos del Estado
RMSE	root mean square error
$RMSE_{peaks}$	RMSE evaluated only at high- and low-tide peaks
$RMSE_{spring}$	RMSE evaluated only at high- and low-tide peaks during spring-tide
$RMSE_{neap}$	RMSE evaluated only at high- and low-tide peaks during neap-tide

Responsible Editor: Juan-Manuel Sayol

✉ Pablo Muñoz-López
pablomlo@uma.es

[1] Physical Oceanography Group, Department of Applied Physics II, University of Málaga, Málaga, Spain

[2] Instituto de Biotecnología y Desarrollo Azul (IBYDA), University of Málaga, Málaga, Spain

[3] Instituto de Ingeniería Oceánica (IIO), University of Málaga, Málaga, Spain

[4] Port Authority of Sevilla, Sevilla, Spain

1 Introduction

Estuaries are dynamic, highly productive ecosystems governed by complex interactions between marine and riverine processes (Savenije 2012). Accurate short-term forecasting of hydrodynamic conditions in these environments is essential for both scientific understanding and applied management. In operational oceanography, forecasting systems that merge real-time observations with numerical models provide a framework to quantify

Published online: 25 February 2026

predictive uncertainty and to support diverse societal applications (Kourafalou et al. 2015).

Over the past decades, operational forecasting systems have become key tools to support estuarine and coastal management worldwide. In South America, real-time forecasting platforms developed for the highly urbanized Santos estuary (Brazil) have shown the value of integrating numerical models and observations to predict short-term water levels and storm tides affecting port operations (Costa et al. 2020; Mendes et al. 2019). Comparable initiatives exist in other regions, including the New York Harbor Observing and Prediction System in North America, which provides real-time water level and circulation forecasts for navigation safety (Georgas et al. 2009; Georgas and Blumberg 2010), and the European Storm Surge Forecasting System, which delivers regional-scale surge predictions for coastal risk management across multiple countries (Fernández-Montblanc et al. 2019). These examples illustrate the growing role of operational forecasting in estuarine environments, where tidal dynamics interact with regulated freshwater inputs and meteorological variability on short timescales (Müller-Navarra and Bork 2011; Kourafalou et al. 2015; NOAA CO-OPS 2020).

Operational forecasting systems may focus on different components of the coastal environment, including hydrodynamics, waves, water quality, and biogeochemical processes, depending on observational availability and management priorities (Kourafalou et al. 2015). Among these, water level forecasting remains a cornerstone of operational estuarine systems due to its direct relevance for navigation safety, flood risk, and coastal management (NOAA CO-OPS 2020).

The Guadalquivir estuary, located in the southwestern Iberian Peninsula, exemplifies a highly regulated, navigable system where hydrodynamic uncertainty has both scientific and practical consequences. The estuary extends approximately 100 km to the Alcalá del Río dam, narrowing from 1 km at its mouth to barely 100 m at its head, with an average channel depth of 6.5 m (Donázar-Aramendía et al. 2018). The 80 km navigable waterway includes the Port of Sevilla (Fig. 1B), the only inland commercial port in Spain. Freshwater discharge, which is heavily regulated by human

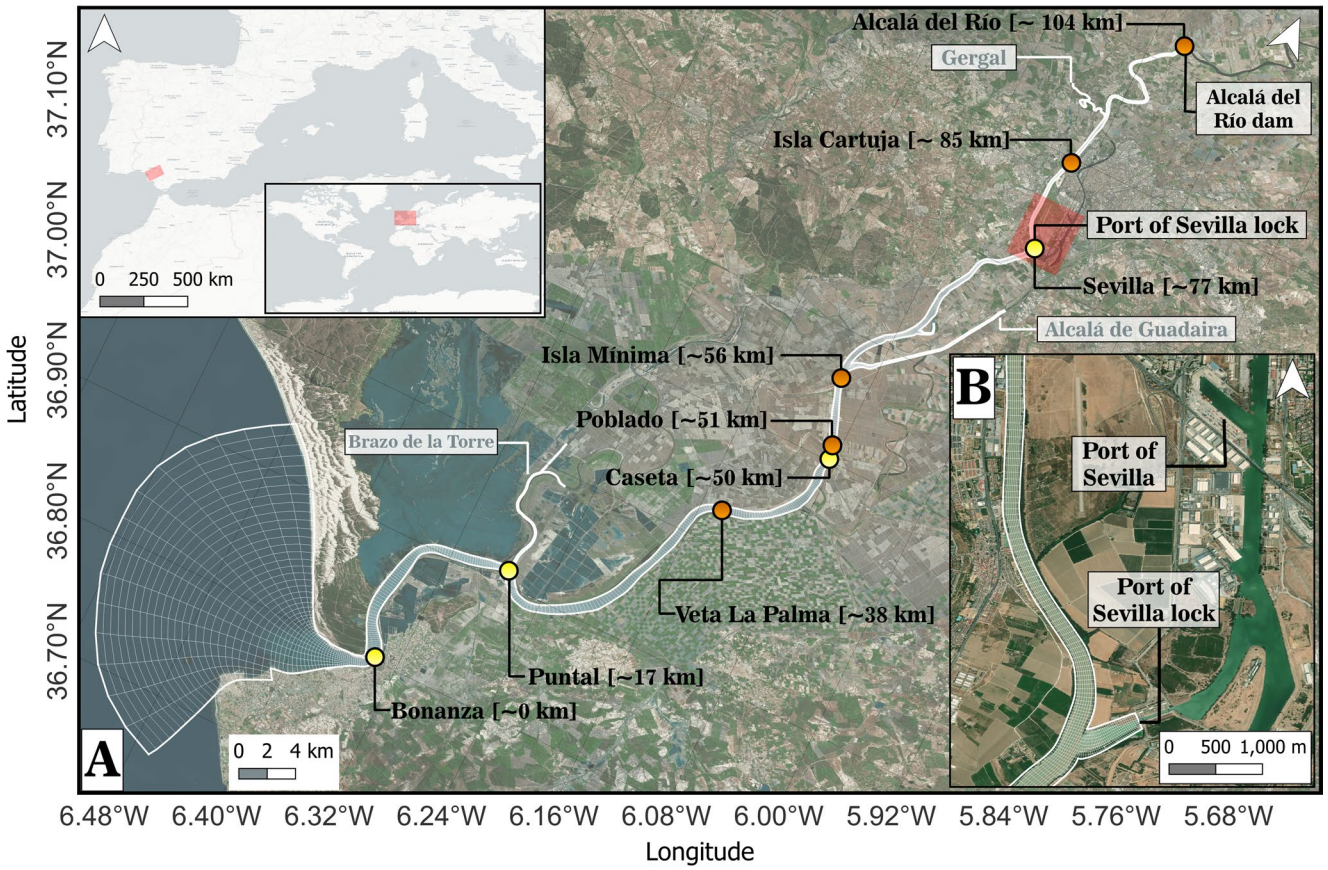

Fig. 1 (**A**) Map of the Guadalquivir estuary displaying the Delft3D computational grid and the tide-gauge observation sites of PdE (yellow circles) and SAIH (orange circles). The positions of the Brazo de la Torre, Alcalá de Guadaira and Gergal tributaries, together with the upstream Alcalá del Río dam and the Port of Sevilla, are also marked. (**B**) Enlargement of the grid stretch that connects the estuary with the Port of Sevilla lock

intervention, averages around 20 $m^3 \cdot s$, but can occasionally exceed several thousand $m^3 \cdot s$ during sporadic flood events (Bermúdez et al. 2021). Under typical low-flow conditions, the estuary exhibits a mesotidal regime dominated by the principal lunar tidal constituent M_2 (Álvarez et al. 2001; Díez-Minguito et al. 2012a; Muñoz-López et al. 2024). Human interventions—including river regulation, land reclamation, meanders cutoffs, and infrastructure development—have altered the hydrodynamic response (Ruiz et al. 2015; Díez-Minguito et al. 2012a), producing a damped, partly reflected semidiurnal tide whose amplitude changes following a V-shape pattern along the channel (Díez-Minguito et al. 2012b, 2013; Muñoz-López et al. 2024). Climate change and future morphological interventions could intensify these alterations (Couto et al. 2024). Recent numerical studies on tidal propagation and resonance dynamics in the Guadalquivir Estuary (Siles-Ajamil et al. 2019; Muñoz-López et al. 2024) further highlight the need for robust, short-term forecasting systems that can be embedded within real-time operational workflows.

In the Guadalquivir Estuary, the implementation of an operational forecasting system is particularly critical due to its navigational, agricultural, and environmental constraints. In this context, accurate short-term water level forecasts are particularly critical for navigation through the 80 km tidal waterway upstream of the port, where safe transits depend on reliable under-keel-clearance estimates and on the scheduling of lock operations at the port of Sevilla (Fig. 1B). While the astronomical tide can be predicted years in advance, the meteorological contribution—often only a few centimeters but sometimes much larger—remains uncertain beyond a few days. Forecasts are also valuable for the extensive rice-growing areas bordering the middle and lower estuary, where they support the optimization of freshwater releases and extractions to minimize salinity stress on crops (Moral Ituarte 1993; Muñoz-López et al. 2025). In addition, water level predictions inform dredging campaigns required to maintain channel depth and provide guidance for fisheries and environmental management in the region (Ruiz et al. 2015).

Against this background, this study presents the development and implementation of an operational real-time hydrodynamic forecasting system for the Guadalquivir Estuary. The system provides 72-h water level forecasts updated twice daily, integrating astronomical tides and meteorological forcing, and is validated against a network of tide gauge observations.

The paper describes the operational framework, its skill assessment, and the strategies adopted to address uncertain forcings. Although the model also resolves velocity, temperature, and salinity fields, the current lack of systematic real-time observations for these variables limits their operational validation, which is discussed together with future extensions of the system.

2 Methodology and system architecture

2.1 Observational data sources

Water level observations from nine tide gauge stations provide spatially representative coverage of the Guadalquivir estuary. Four radar gauges belonging to the Puertos del Estado (PdE, hereinafter) REDMAR network (yellow dots in Fig. 1A) are located along the navigable reach, and their data are freely accessible at https://portus.puertos.es. Additionally, the Automatic Hydrological Information System for river flood management (SAIH hereinafter, https://www.chguadalquivir.es/saih), belonging to Guadalquivir Hydrographic Confederation, provides five real-time gauges in the middle and upper estuary (orange dots in Fig. 1A). For the present analysis, we use the seven stations that remained fully operational throughout 2024; the Puntal and Caseta gauges, which were intermittently offline, were excluded (see Fig. S1 of the Supplementary Material), following the quality-control criteria described in Muñoz-López et al. (2024). These data are systematically collected via automated protocols and databases provided by regional monitoring networks.

Discharges observations are also supplied by SAIH. Approximately 80% of the total inflow originates from the Alcalá del Río dam (Bermúdez et al. 2021), with an average release of 20 $m^3 \cdot s$, while the Brazo de la Torre, Alcalá de Guadaira, and Gergal tributaries contribute approximately 0.35, 0.75, and 0.80 $m^3 \cdot s$, respectively.

2.2 Numerical model configuration

The operational forecasting system employs the Delft3D hydrodynamic model, the same model as in Muñoz-López et al. (2024, 2025). A detailed description can be found in those studies; here we summarize the main aspects relevant to the present implementation. The Delft3D-Flow software package (Deltares 2022) is a robust, widely used numerical modeling tool capable of solving three-dimensional shallow-water and transport equations. The computational domain extends from 5° 58′ W to 6° 34′ W and from 36° 39′ N to 37° 31′ N (Fig. 1A), discretized with a curvilinear grid following the Arakawa-C scheme and a vertical sigma-coordinate system of ten layers. Horizontal resolution ranges from ~300 m in the ocean to a few meters in the tributaries. Bathymetry is provided by the Port of Sevilla. Along the 80-km navigable reach, it is surveyed frequently, yielding very detailed and regularly updated bathymetry,

whereas upstream of Sevilla, where commercial traffic is absent, bathymetric data is older and sparser, introducing higher modelling uncertainty. A detailed visualization of the numerical bathymetry is shown in Fig. S2 of the Supplementary Material.

Background horizontal viscosity and diffusivity have been set to 1 m²/s and 10 m²/s, respectively (Deltares 2022), while no background values were used for the vertical components. Bottom stress was represented using the 3D formulation of the Chézy friction coefficient, which is directly linked to the riverbed roughness length k_s (see Muñoz-López et al. 2024 for details). A constant roughness length of $k_s = 1.5 \times 10^{-4}$ m for all the domain, provide the best agreement between model outputs and observations under low-discharge conditions.

The model integrates multiple forcings:

- Astronomical tide imposed at the ocean boundary using harmonic constants (Muñoz-López et al. 2024).
- Meteorological tide retrieved from the operational NIVMAR model (Álvarez Fanjul et al. 2001) at the ocean boundary, which is used as sub-inertial water level corrections.
- Temperature (20-year daily average from SAIH) and salinity (36.7 g/kg at the mouth; 0.1 g/kg for freshwater) are set as boundary conditions.
- Wind stress and atmospheric and radiative forcing at the free surface data retrieved from the operational HARMONIE-AROME numerical weather prediction model (Ruiz Pacheco et al. 2018) operated by the Spanish State Meteorological Agency and interpolated to the spatial grid.
- Freshwater discharges in the cells attached to freshwater sources (see Fig. 1A).

To enhance computational efficiency and operational usability, the model runs in parallelized mode. The main $924 \times 375 \times 10$ nodes regular domain is split into 12 subdomains (see Fig. S3 of the Supplementary Material), which keep approximately the same number of nodes to be computed. This parallelization reduces run time by a factor of ~37 compared to the non-parallel configuration. Each tile runs on a single thread and provides the real-time boundary conditions for the adjacent tiles, while additional threads coordinate communication and file output. The model is executed on a high-performance computing machine with 24 physical cores, 64 GB RAM, 8 GB GPU capacity.

2.3 Model calibration and validation

The calibration of the hydrodynamic model follows the methodology established by Muñoz-López et al. (2024), using an identical model configuration, which is briefly summarized here. Harmonic analysis was performed on the available water level observations, and the resulting harmonic constants were compared to those derived from the numerical model. Differences in the amplitude of the dominant M_2 tidal constituent were less than 3 cm throughout the estuary, with phase discrepancies under 10 min (see Fig. 2 in Muñoz-López et al. 2024). Model performance was further assessed using time series of observed and simulated water levels at two monitoring stations situated in the lower and upper reaches of the navigable stretch of the Guadalquivir estuary (see locations in Fig. 1, Muñoz-López et al. 2024). Agreement was high, with Pearson correlation coefficients of 0.981 and 0.985, and root mean square errors (RMSE) of 1.3 cm and 1.1 cm, respectively. Velocity data collected at an intermediate estuarine location, also showed strong agreement with model results, with RMSE values below 5 cm/s (see Fig. 3 in Muñoz-López et al. 2024). These measurements were obtained during a dedicated field campaign and are therefore not available in real time. The salinity component of the model has also been satisfactorily validated in Muñoz-López et al. (2025), further supporting the robustness of the model configuration and its suitability for simulating hydrodynamic processes in the Guadalquivir estuary.

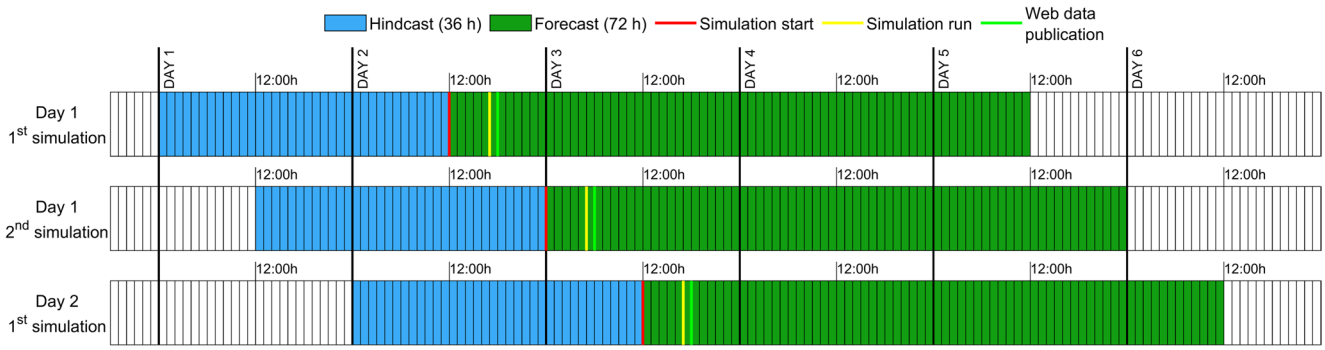

Fig. 2 Schematic representation of the temporal distribution of model simulations. Each simulation includes a 36-h hindcast (blue shade) and a 72-h forecast (green shade), executed every 12-h. The diagram also indicates the timing of model initialization (red line), execution (yellow line), and publication of forecast outputs (light green line) on the web platform

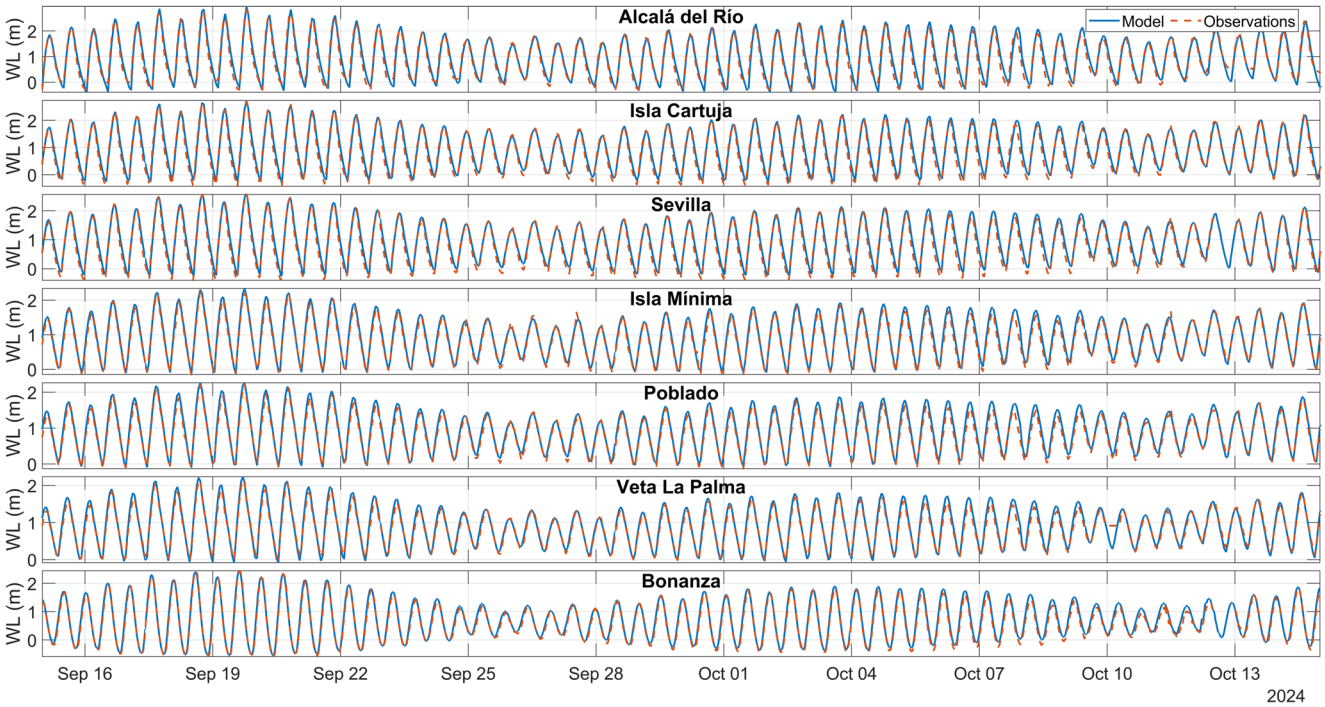

Fig. 3 Comparison of the water level modeled by the operational model (solid blue) and the observed level (dashed orange) for the period 15 September – 15 October 2024

Model performance should be interpreted considering the underlying bathymetric features, which play a fundamental role in estuarine hydrodynamics. In systems such as the Guadalquivir Estuary, bathymetry is not only spatially heterogeneous but also temporally variable due to anthropogenic interventions and natural sediment dynamics (Ruiz et al. 2015; Megina-Martínez et al. 2023). The consistency between the bathymetry used by the model and the actual bathymetric conditions during the observation period is therefore a key factor controlling validation results. When the model is forced with outdated bathymetry, both model skill and the harmonic characteristics of the observed signal may be affected, particularly in the upper estuary where bathymetric surveys are less frequent. Conversely, once the model is calibrated, local bathymetric modifications such as maintenance dredging have a comparatively irrelevant impact on the overall consistency of the hydrodynamic solutions, as shown by additional sensitivity analyses included in Section S2 of the Supplementary Material. Nevertheless, other types of morphological alterations, such as the opening of new channels or the reconnection of the estuary with adjacent tidal flats, may locally affect tidal dynamics and cannot be considered negligible (Siles-Ajamil et al. 2019; Muñoz-López et al. 2025). In addition, flood events can substantially modify the fluvial regime by redistributing sediments and inducing bathymetric changes, thereby influencing estuarine dynamics both during and after the event (Losada et al. 2017).

2.4 Operational forecasting workflow

The operational configuration distinguishes between externally-supplied forcings, integrated in real time from external providers, and internally-prescribed forcings that can be generate without outside input. The latter group includes the astronomical tide imposed at the ocean boundary and the climatological temperature and salinity fields applied at the open boundaries. The externally-supplied forcings comprise the meteorological tide from NIVMAR, regulated freshwater releases at the Alcalá del Río dam and the main tributaries provided from the SAIH, and the surface wind and heat-flux fields delivered by the HARMONIE-AROME atmospheric forecast.

The model runs automatically every 12-h using a leapfrog temporal structure, consisting of a 36-h hindcast (retrospective simulation) and a 72-h forecast (forward simulation), as illustrated in Fig. 2. This configuration is synchronized with the operational cycle of the NIVMAR model, from which the 72-h forecast meteorological contribution is obtained. Custom algorithms ensure robustness in the integration of external data and handle potential gaps in forcing inputs. For instance, if meteorological tide data are unavailable likely due to NIVMAR failure, the algorithm replaces the missing segment with a zero-valued fictitious series. Atmospheric forcing from HARMONIE-AROME is available for the first 48-h; the remaining 24-h are filled by repeating the last available day of radiative forcing, while wind is

set to zero. Freshwater inputs are used up to real-time and extended into the forecast period using the mean value of the 36-h hindcast period. This strategy ensures continuous and uninterrupted model operation.

In Fig. 2, the red line indicates the start of the automated workflow. Four hours later (yellow line), after a buffer period set to ensure that all external providers (NIVMAR, HARMONIE-AROME and SAIH) have completed their latest cycles and published the required data, the simulation is run. Following the simulation, post-processing and quality-control routines are applied, and the resulting products are uploaded to the web interface (light green line) in less than one hour. The entire workflow, from data collection to web publication, requires ~35 min of computational time.

2.5 Forecast outputs and skill assessment

Every 12-h cycle, the operational system produces a full 72-h water level forecast on the model grid and at seven tide gauges where real-time observations are available. Although the model also provides three-dimensional velocity, temperature, and salinity fields (Muñoz-López et al. 2024, 2025), only water level forecasts are currently disseminated in this initial operational release. At present, operational forecast verification is therefore limited to water level, as no real-time current velocity observations are available in the estuary. The additional 3D variables are archived internally for potential future integration. Forecast verification is performed for each simulation and structured around three components that provide quantitative skill metrics:

- **Direct water level comparison**. One month of operational output is compared with observations from the seven tide-gauge stations. The selected interval, 15 September – 15 October 2024, chosen here as an illustrative example, corresponds to a period with complete records and without major flood pulses that could disturb the tidal regime.
- **Bulk statistics**. Root-Mean-Square Error (RMSE) and the Pearson correlation coefficient (r) are computed following the framework described by Costa et al. (2020). In addition, three complementary metrics are introduced to better characterize errors at tidal extremes: $RMSE_{peaks}$, defined as the RMSE evaluated only at high- and low-tide peaks; $RMSE_{spring}$, computed considering only peaks during spring-tide periods; and $RMSE_{neap}$, computed analogously for neap-tide periods. These metrics help to disentangle phase-lag and amplitude-related errors and to assess model performance under different tidal-energy conditions. To facilitate comparison across stations with different tidal amplitudes, error metrics are expressed both in absolute terms and as normalized values. RMSE computed over the full time series is normalized by the tidal range over a reference period with complete or nearly complete data at all stations (2022–2023; see Fig. S1 of the Supplementary Material), while $RMSE_{peaks}$ is normalized by the mean observed high-tide peak height over the same reference period.
- **Alert thresholds**. During every hindcast cycle, if RMSEpeaks at Bonanza (mouth), which is the tide gauge offering the longest and more robust time series, exceeds 12.5?cm or if r falls below 0.9, the run is flagged, and an automatic email alert is sent to system operators. This threshold-based monitoring transforms forecast verification into a real-time quality-control process.

All forecasts, observations, and skill scores are archived systematically, enabling retrospective evaluation and progressive refinement of the forecasting system.

3 Results

This section presents an evaluation of the operational model performance. We first assess water level forecast skill over a one-month evaluation period using bulk statistical metrics. We then examine four consecutive 72-h forecasts cycles covering a 20-day operational period, in order to illustrate phase coherence and amplitude accuracy at representative sites. A sensitivity experiment evaluates the robustness of the system to uncertain forcings. Finally, we summarize the alert thresholds implemented in the system, indicating when they are triggered and the conditions that cause the alerts.

3.1 Forecast skill assessment

3.1.1 Validation against tide gauges

Figure 3 compares observed (dashed orange line) and simulated (solid blue line) water levels at seven tide-gauge sites along the Guadalquivir Estuary, from the closure dam at Alcalá del Río to the mouth at Bonanza, over a continuous 30-day period. The operational model reproduces the semidiurnal tidal signal and spring–neap modulation with high fidelity across the estuary, with only minor amplitude differences at the two most upstream stations.

The corresponding skill metrics are summarized in Table 1. Model error increases gradually in the upstream direction, with RMSE values ranging from 11.8 cm at Bonanza (6.6% of the local tidal range) to 19.9 cm at Alcalá del Río, corresponding to a maximum relative error of approximately 10% of the tidal range. Errors evaluated at tidal extremes remain moderate, with $RMSE_{peaks}$ below the 15 cm alert threshold at all stations and normalized

Table 1 Root-Mean-Square error (RMSE) computed over the complete time series, normalized RMSE (N_{RMSE}), pearson correlation coefficient (r), RMSE evaluated at high- and low-tide peaks ($RMSE_{peaks}$) and its normalized value ($N_{RMSEpeaks}$), together with RMSE values computed separately for representative spring-tide ($RMSE_{spring}$) and neap-tide ($RMSE_{neap}$) periods, at each tide-gauge station for the period 15 September–15 October 2024

Stations	RMSE (cm)	N_{RMSE} (%)	r	$RMSE_{peaks}$ (cm)	$N_{RMSEpeaks}$ (%)	$RMSE_{spring}$ (cm)	$RMSE_{neap}$ (cm)
Alcalá del Río	19.9	10.0	0.971	14.9	7.6	13.4	12.9
Isla Cartuja	18.2	8.8	0.979	10.9	7.1	10.9	10.8
Sevilla	17.4	9.0	0.985	12.9	8.7	11.2	13.0
Isla Mínima	10.8	6.9	0.991	8.6	6.9	5.1	9.3
Poblado	11.9	8.6	0.991	9.8	7.4	7.5	7.8
Veta La Palma	10.6	7.8	0.987	7.9	8.9	6.9	7.6
Bonanza	11.8	6.6	0.994	8.6	3.7	5.2	4.9

differences consistently below 9%, with an average value of 7.1%. Comparable or slightly lower error levels are obtained when RMSE is computed separately for spring ($RMSE_{spring}$) and neap ($RMSE_{neap}$) tide conditions. Finally, Pearson correlation coefficients are consistently high ($r \geq 0.97$), indicating strong phase agreement between modeled and observed water levels. Overall, these results demonstrate that the operational system maintains robust performance across different tidal regimes.

Figure 4 illustrates four consecutive 72-h forecasts (colored lines) and corresponding observations (black line) at three representative stations: Sevilla (upper reach), Veta La Palma (middle reach), and Bonanza (lower reach). Each forecast begins after its 36-h hindcast (vertical markers), together spanning a 20-day period of continuous operation. Forecasts remain phase-locked with observations, without discernible timing drift, even at the upstream limit of navigation (Sevilla). Peak-to-trough tidal ranges are accurately

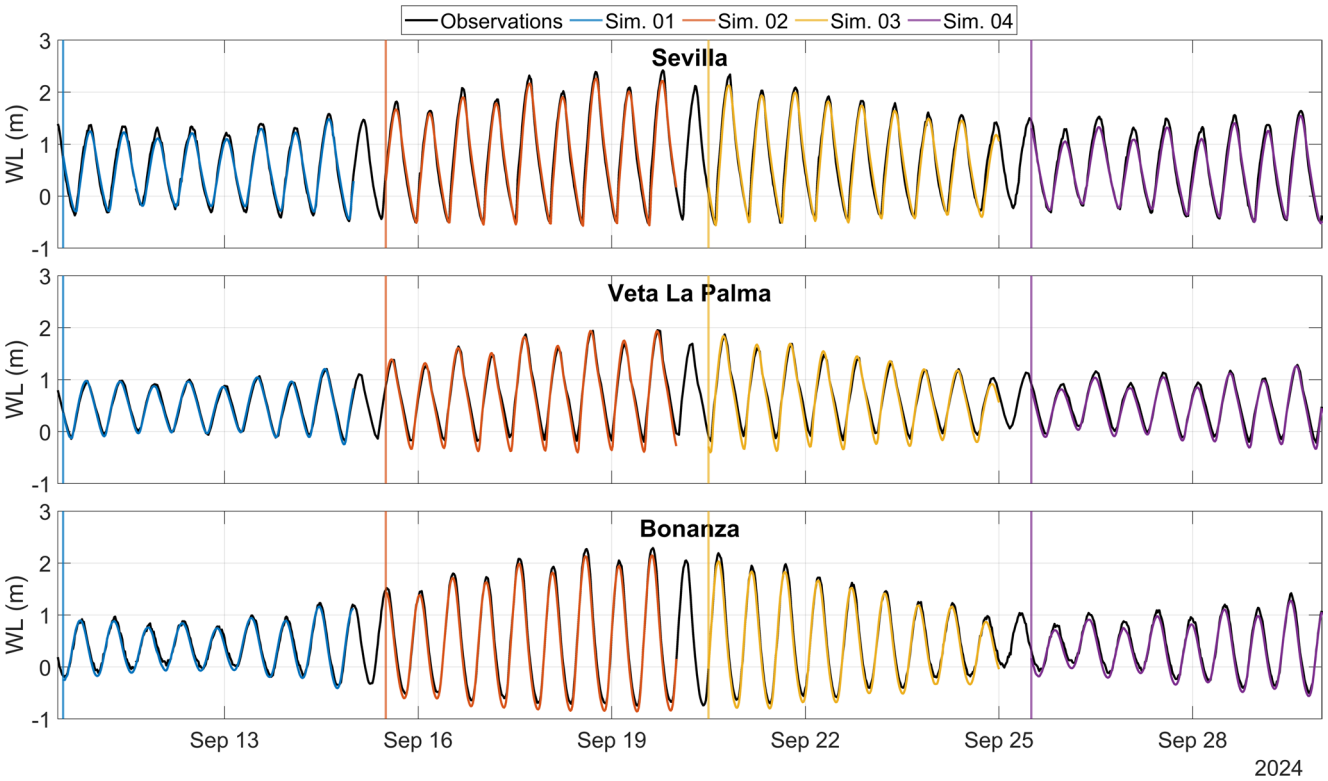

Fig. 4 Direct comparison of observed water levels (black line) and simulated water levels (colored lines) from four test simulations over a 20-day operational period at three tide gauges that represent the navigable part of the Guadalquivir estuary. Each simulation includes a 36-h hindcast followed by a 72-h forecast. Vertical lines indicate the forecast start times. Sevilla is used as the upstream reference rather than Alcalá del Río, since the operational system is intended as a navigation-support tool and the estuary ceases to be navigable for large vessels upstream of the Port of Sevilla lock system (see Fig. 1B). The remaining tide gauges exhibit similar results and are therefore included only in the Supplementary material (Fig. S4)

captured, typically within ±10 cm at Bonanza and Veta La Palma and within ±13 cm at Sevilla. These findings are consistent with Table 1, where the mean $RMSE_{peaks}$ remains below 15 cm and the Pearson correlation exceeds 0.97 for all forecasts. This skill is spatially homogeneous and does not deteriorate from one forecast cycle to the next, confirming that the current operational configuration setup provides stable and reliable 72-h water level predictions.

3.1.2 Robustness to uncertain forcings

Operational forecasts require assumptions for forcings beyond the nowcast window. Dam releases are fixed at their 36-h hindcast average, and wind fields are set to zero beyond 48-h. To test the sensitivity of this approach, an experiment was performed where observed discharge and wind were imposed over the full 72-h forecast horizon (Fig. 5).

Results indicate that discharge variability of 0–30 $m^3 \cdot s^{-1}$ (instead of the constant 9 $m^3 \cdot s^{-1}$ mean) modifies water levels by ±4 cm near the dam (light grey line in Fig. 5A), a signal attenuated to <2 cm at Isla Mínima (light grey line in Fig. 5B) and negligible downstream. Suppressing moderate 5–10 $m \cdot s^{-1}$ winds beyond 48-h introduces differences <1 cm at Bonanza (light grey line after hour 14:00 in Fig. 5C). These results demonstrate that forecast skill is only marginally affected by these simplified boundary assumptions, confirming the robustness of the operational strategy.

3.2 Automated alerting system

Forecasts are complemented by an internal alerting protocol. At the end of each cycle, two indicators are evaluated at Bonanza tide gauge (PdE network): $RMSE_{peaks}$ and Pearson correlation (r) computed over the observed and modeled hindcast water level series, both indicators already used for the validation in Section 3.1.1.

If either indicator falls outside established thresholds ($RMSE_{peaks} > 12.5$ cm or $r < 0.9$) the simulation is automatically flagged on the diagnosis files, and an email is sent to the duty forecaster. The 12.5 cm tolerance corresponds to an internal operational criterion derived from long-term statistics at both stations: it represents roughly 8–10% of the typical spring-tide range in mid-estuary, making it sensitive enough to detect meaningful forecast degradations, yet large enough to avoid false alarms caused by sensor noise. The 0.9 correlation threshold helps identify the remaining failures due to severe phase shifts between the observed and modeled outputs, which the $RMSE_{peaks}$ metric often masks.

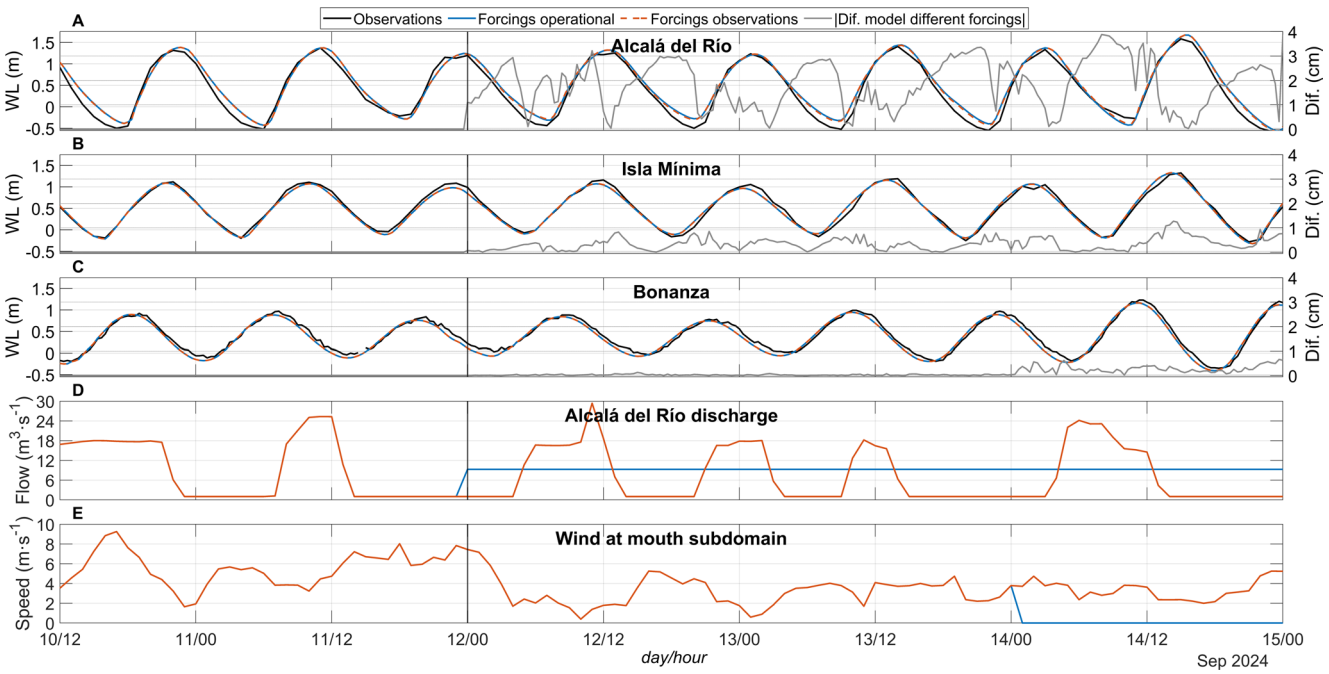

Fig. 5 Panels **A**–**C** compare observed water levels (black line) with two model runs at three representative tide gauge stations: Blue line is the output of the operational configuration used in daily production, whereas dashed orange line is the output of a sensitivity run in which observed wind and dam discharge are applied for the full 72-h instead of being replaced by the hindcast period mean (discharges) and zero-wind assumption beyond 48-h (see text for details). Light grey curves show the absolute difference between the two runs (scale on the right axis). Panel **D** shows the time-dependent discharge released at the Alcalá del Río dam used in the sensitive run (orange line) and the hindcast period mean value routinely applied in the operational forecast window (blue line). Panel **E** shows the observed wind speed used in the sensitive run (orange line) and the operational zero-wind assumption beyond the first 48-h (blue line)

3.2.1 Frequency of alerts

Between 30 April 2024 and 25 June 2025, 843 forecast cycles were completed, generating 94 alerts (≈11% of runs). These alerts fall into three categories:

- Major river discharges (>200 $m^3 \cdot s^{-1}$ at Alcalá del Río) that abruptly alter the water column inducing a regime shift likely due to high-suspended sediment concentrations that discharge triggers and distort the tidal dynamics (<3.5% of all alerts).
- Sustained winds (>10 $m \cdot s^{-1}$), typically during storms and peak discharges, destabilizing water level signals (<1.5%).
- Unexplained or isolated events, likely related to sensor fouling or accidental disturbance (<7%).

Thus, ~40% of the warnings can be traced to well-defined hydrometeorological forcings, while the remainder likely reflects a combination of undocumented sensor anomalies and residual model limitations These results highlight the importance of further calibration and development of advanced quality-control filters. At the same time, they confirm that the present thresholds are selective, scientifically justified, and operationally effective.

4 Discussion and conclusions

4.1 Discussion

The Guadalquivir operational forecasting system achieves operational skill levels comparable to, or in some respects exceeding, those reported for other estuarine forecasting services (Müller-Navarra and Bork 2011; Elbe estuary, Germany; Costa et al. 2020; and Mendes et al. 2019; Santos estuary, Brazil), supporting reliable decision-making in navigation and logistics. Forecast accuracy tends to decrease slightly toward the estuary head, a pattern attributable to the coarse bathymetric data in the upper reaches. Under typical low-discharge conditions (less than 200 $m^3 \cdot s^{-1}$) $RMSE_{peaks}$ remains below 15 cm across the estuary, and below 10 cm within the navigable reach. These values represent only 6–10% of the characteristic tidal range in the mid-estuary, confirming that predictions meet the accuracy required for operational applications.

The harmonic constituent analysis corroborates these bulk statistics. The dominant semidiurnal tide is accurately reproduced, whereas greater scatter occurs in diurnal and overtide constituents, particularly at the estuary head where tidal reflection and non-linear distortion from enhanced friction are strongest (Díez-Minguito et al. 2012a, b; Muñoz-López et al. 2024). However, these secondary components are almost an order of magnitude weaker than the prevailing M_2, and their contribution to water level prediction error is operationally negligible, particularly downstream of Sevilla, where the discrepancies become even smaller. No systematic timing drift was detected between successive 12-h forecast cycles, indicating that spatial consistency and temporal stability are preserved throughout the 72-h forecasts. Taken together, these results demonstrate that the present operational configuration provides stable, accurate water level predictions suitable for real-time operational applications in the Guadalquivir estuary.

Sensitivity tests demonstrate that the treatment of unknown future forcings (i.e., dam discharge held at its hindcast mean and zeroing wind stress beyond 48-h) adds errors of less than 4 cm in predicted water levels, well inside the system's intrinsic uncertainty envelope. Therefore, for short forecasts (less than 72-h) under usual low-discharge conditions, the lack of a fully deterministic discharge or a high-precision 72-h wind forecast does not significantly affect the accuracy of the water level prediction, thus confirming the robustness of the system under uncertain inputs. Consequently, the operational system supplies reliable water-level forecasts for port-specific activities, such as optimizing each vessel's transit, selecting entry and departure times and adjusting speed in each reach, or defining dredging windows for channel maintenance.

Although the Guadalquivir estuary operational system meets accuracy targets under the low-discharge regime (<200 $m^3 \cdot s^{-1}$) that prevails for more than 70% of the year (Losada et al. 2017), the estuary is also subject to short-duration river pulses that can exceed 400 $m^3 \cdot s^{-1}$ at the Alcalá del Río (Bermúdez et al. 2021). Field evidence shows that such events inject very high suspended-sediment concentrations, which in turn increase vertical stratification and amplify the tidal signal, sometimes preventing a full return to pre-flood baseline levels (Wang et al. 2014; Losada et al. 2017). Comparable challenges have been documented in other estuaries, such as the Santos estuary (Brazil), where Mendes et al. (2019) highlighted the importance of updating discharge inputs and bottom-stress parameterization to preserve forecast skill during floods. For the Guadalquivir estuary, a similar operational strategy will likely be required: when dam releases exceed a configurable threshold (e.g., 400 $m^3 \cdot s^{-1}$), transitioning to a high-turbidity regime through adjustment of bottom-roughness coefficients will be essential to maintain forecast reliability, particularly during extreme events when robust guidance is most critical.

4.2 Limitations

Few limitations qualify the present findings:

- The current operational configuration is developed for low-to-moderate freshwater discharges (less than 200 $m^3 \cdot s^{-1}$) which dominate the Guadalquivir estuary. However, major flood releases (more than 400 $m^3 \cdot s^{-1}$) can rapidly increase suspended-sediment concentrations, alter vertical stratification and, therefore, require event-specific retuning of bottom-friction and turbidity-related parameters.
- Treatment of river discharges is simplified: beyond the hindcast window the model assumes constant mean values. This pragmatic strategy has been shown to preserve forecast skill under the low-to-moderate discharge conditions that dominate the system, but forecast reliability decreases when dam releases deviate markedly during short-lived high-flow events. Access to short-term (e.g., 2-day) discharge forecasts from the basin authority (SAIH) would therefore improve performance during such severe episodes.
- Bathymetric data in the upper reaches upstream of Sevilla are sparse, forcing a coarse mesh representation that partly explains the larger discrepancies in simulated water level near Alcalá del Río dam.
- Real-time gauge data occasionally contain gaps or spurious spikes (UNESCO-IOC 2020). Although obvious outliers are manually filtered, residual errors can still affect short validation windows.
- The present configuration neglects wind forcing beyond 48-h and does not include sediment-transport or biogeochemical modules. These omissions are consistent with the short-range, water level forecasting focus of the system and do not compromise its hydrodynamic skill. However, they restrict direct applicability to morphodynamic or ecological studies, where extended forcings and coupled processes would be required.

Taken together, these simplifications constrain the system's applicability for environmental-quality and morphodynamic studies under high-discharge conditions, but remain fully acceptable for short-range operational water level forecasting, which is the primary focus of the present study.

4.3 Conclusions

The operational forecasting system developed for the Guadalquivir estuary fulfils—and in many respects surpasses—the accuracy requirements not only for short-term navigation guidance but also for broader applications in operational oceanography and estuarine management:

- **Forecast skill for decision support.** The root-mean-square error evaluated only at high- and low-tide peaks ($RMSE_{peaks}$) in predicted water level remains below 15 cm throughout the estuary, and under 10 cm within the navigable reach (Table 1), only 6–10% of the representative tidal range in the mid-estuary, providing ample safety margins under the low-discharge regime that prevails for more than 70% of the year.
- **Temporal stability.** No systematic timing drift is detected between successive 12-h forecast cycles. The 72-h predictions maintain accurate space-time coherence of the dominant semidiurnal tide throughout the estuary, demonstrating the robustness of the operational configuration.
- **Treatment of unknown forcings.** Holding river discharge at its hindcast mean during the forecast and zeroing wind stress beyond 48-h introduces some additional uncertainty, but the impact on predicted water level is always smaller than 4 cm, well inside the model's intrinsic uncertainty, demonstrating that this pragmatic approach is adequate for short-term water level forecasting.

Taken together, these results demonstrate that the forecasting system—integrating the hydrodynamic core, forcing strategy, and automated alert protocol—provides a reliable real-time decision-support tool for the Guadalquivir estuary under typical low-discharge conditions. Its modular architecture represents a transferable reference for operational estuarine forecasting worldwide, bridging physical modeling with applied oceanography.

4.4 Future work and integration opportunities

The present water level centered operational framework should be regarded as a nucleus rather than an end point. In line with the call by Kourafalou et al. (2015) for "continuous development of innovative methodologies and tools" in coastal-shelf forecasting, several forthcoming extensions could further enhance the Guadalquivir estuary operational system:

- **Enhanced observational network.** Densification of the monitoring system through radar gauges and bottom-mounted current profilers would close spatial gaps, improve model calibration, and facilitate early detection of forecast drifts. In this context, the Port of Sevilla is currently working to expand the observational component of the operational system, including the deployment of real-time current measurements, which will enable systematic validation of modeled velocities in future system updates.

- **Discharge forecast integration.** Coupling the model with short-term regulated-release schedules, upstream reservoir operations, or catchment precipitation forecasts would provide more realistic ensembles of freshwater input scenarios, improving predictive skill during high-flow events.
- **Expanded variable validation**. Systematic validation of currents, salinity, and temperature would extend confidence in the model beyond water levels, enabling a more comprehensive representation of estuarine dynamics.
- **Operational readiness and extensibility.** Beyond its demonstrated hydrodynamic skill, the forecasting system has been designed with a modular architecture that enables the future integration of visualization tools and decision-support layers. A prototype web-based interface illustrating this potential is described in Section S3 of the Supplementary Material, while the present study deliberately focuses on the validation of the hydrodynamic core and its operational robustness.
- **Coupled process modeling.** Linking the hydrodynamic core with sediment-transport modules (Deltares 2022) and Lagrangian-drift models (Dagestad et al. 2018) would support applications to morphodynamic evolution and dispersal of sediments or pollutants.
- **Automated quality control.** Implementing real-time algorithms to flag or discard anomalous gauge readings prior to statistical evaluation would prevent spurious spikes—often induced by sensor noise, clock drift, or temporary fouling (UNESCO-IOC 2020)—from distorting performance metrics.

Together, these enhancements would not only reinforce the robustness of the Guadalquivir estuary operational system but also position it as a flexible framework for estuarine forecasting more broadly, aligned with international efforts in operational oceanography.

Supplementary Information The online version contains supplementary material available at https://doi.org/10.1007/s10236-026-01778-8.

Acknowledgements We thank the Guadalquivir Hydrographic Confederation, through its SAIH system, for making freely available both the water-level data used to calibrate and validate the numerical model and the records of regulated freshwater releases at the Alcalá del Río dam and the main tributaries that feed the operational model. We are also grateful to Puertos del Estado for providing access to additional water-level observations for model validation and for freely distributing the meteorological tide generated by the NIVMAR model. Finally, we thank Universidad de Málaga for funding for open access charge.

Author contributions PML: Conceptualization, Data curation, Formal analysis, Investigation, Methodology, Software, Validation, Visualization, Writing – original draft. SS: Conceptualization, Formal analysis, Software, Visualization, Supervision, Writing – review & editing. JGL: Conceptualization, Formal analysis, Funding acquisition, Project administration, Writing – review & editing. IN: Formal analysis, Software, Visualization, Writing – review & editing. AB: Funding acquisition, Project administration, Resources. AP: Funding acquisition, Project administration, Resources.

Funding Funding for open access publishing: Universidad de Málaga/CBUA. Financial support from the Port Authority of Sevilla project 2020-ES-TM-0038-S (Optimization of the accessibility conditions) through the Connecting Europe Announcement (2020) is acknowledged. PML acknowledges the contract ascribed to this project. Funding for open access charge: Universidad de Málaga/CBUA.

Data availability No datasets were generated or analysed during the current study.

Declarations

The authors declare that the research was conducted in the absence of any commercial or financial relationships that could be construed as a potential conflict of interest.
During the preparation of this work, the author(s) used ChatGPT in the writing process to improve the readability and language of the manuscript. After using these tools, the author(s) reviewed and edited the content as needed and take(s) full responsibility for the content of the published article.

Competing interests The authors declare no competing interests.

Clinical trial number Not applicable.

References

Bermúdez M, Vilas C, Quintana R, González-Fernández D, Cózar A, Díez-Minguito M (2021) Unraveling spatio-temporal patterns of suspended microplastic concentration in the Natura 2000 Guadalquivir estuary (SW Spain): observations and model simulations. Mar Pollut Bull 170:112622. https://doi.org/10.1016/j.marpolbul.2021.112622

Costa CGR, Leite JRB, Castro BM et al (2020) An operational forecasting system for physical processes in the Santos–São Vicente–Bertioga estuarine System, Southeast Brazil. Ocean Dyn 70:257–271. https://doi.org/10.1007/s10236-019-01314-x

Couto I, Picado A, Des M et al (2024) Climate change and tidal hydrodynamics of guadalquivir estuary and Doñana marshes: a comprehensive review. J Mar Sci Eng 12:1443. https://doi.org/10.3390/jmse12081443

Dagestad KF, Röhrs J, Breivik Ø, Ådlandsvik B (2018) OpenDrift v1.0: a generic framework for trajectory modelling. Geosci Model Dev 11:1405–1420. https://doi.org/10.5194/gmd-11-1405-2018

Deltares (2022) Delft3D-FLOW: simulation of multi-dimensional hydrodynamic flows and transport phenomena, including sediments. User Manual, Hydro-Morphodynamics, version 3.15, SVN rev, vol 57696. Deltares, Delft

Díez-Minguito M, Baquerizo A, Ortega-Sánchez M, Navarro G, Losada M (2012a) Tide transformation in the guadalquivir estuary (SW Spain) and process-based zonation. J Geophys Res Oceans 117:C03019. https://doi.org/10.1029/2011JC007344

Díez-Minguito M, Baquerizo A, Ortega-Sánchez M, Ruiz I, Losada MÁ (2012b) Tidal wave reflection from the closure dam in the guadalquivir estuary. Coast Eng Proc 33:currents58. https://doi.org/10.9753/icce.v33.currents.58

Donázar-Aramendía I, Sánchez-Moyano JE, García-Asencio I, Miró JM, Megina C, García-Gómez JC (2018) Maintenance dredging impacts on a highly stressed estuary (Guadalquivir Estuary): a baci approach through oligohaline and polyhaline habitats. Mar Environ Res 140:455–467. https://doi.org/10.1016/j.marenvres.2018.06.009

Fernández-Montblanc T, Vousdoukas MI, Ciavola P, Voukouvalas E, Mentaschi L, Breyiannis G, Feyen L, Salamon P (2019) Towards robust pan-European storm surge forecasting. Ocean Model 133:129–144. https://doi.org/10.1016/j.ocemod.2018.12.001

Georgas N, Blumberg AF (2010) Establishing confidence in marine forecast systems: the design and skill assessment of the New York Harbor Observation and Prediction System, version 3 (NYHOPS v3). In: *Proceedings of the 11th International Conference on Estuarine and Coastal Modeling (ECM11)*, ASCE, Seattle, pp 660–685

Georgas N, Blumberg AF, Bruno MS, Runnels DS (2009) Marine forecasting for the New York urban waters and harbor approaches: the design and automation of NYHOPS. In: *Proceedings of the 3rd International Conference on Experiments/Process/System Modelling, Simulation and Optimization*, Athens, vol 1, pp 345–352

Kourafalou V, De Mey P, Staneva J, Ayoub N, Barth A, Chao Y, Cirano M, Fiechter J, Herzfeld M, Kurapov A et al (2015) Coastal ocean forecasting: science foundation and user benefits. J Oper Oceanogr 8:147–167. https://doi.org/10.1080/1755876X.2015.1022336

Losada MÁ, Díez-Minguito M, Reyes-Merlo MÁ (2017) Tidal-fluvial interaction in the Guadalquivir River estuary: spatial and frequency-dependent response of currents and water levels. J Geophys Res Oceans 122(2):1384–1406. https://doi.org/10.1002/2016JC011984

Álvarez Fanjul E, Pérez Gómez B, Arévalo I (2001) Nivmar: a storm surge forecasting system for Spanish waters. Sci Mar 65(Suppl 1):145–152. https://doi.org/10.3989/scimar.2001.65s1145

Álvarez O, Tejedor B, Vidal J (2001) La dinámica de Marea En El estuario Del guadalquivir: Un Caso peculiar de «resonancia antrópica». Fís Tierra 13:11–24. https://dialnet.unirioja.es/servlet/articulo?codigo=268752

Megina-Martínez C, Donázar-Aramedía Í, Miró JM, García-Lafuente J, García-Gómez JC (2023) The hyperturbid mesotidal Guadalquivir estuary during an extreme turbidity event: identifying potential management strategies. Ocean Coast Manag 246:106903. https://doi.org/10.1016/j.ocecoaman.2023.106903

Mendes J, Leitão P, Chambel Leitão J, Bartolomeu S, Rodrigues J, Dias JM (2019) Improvement of an operational forecasting system for extreme tidal events in Santos estuary (Brazil). Geosci 9:511. https://doi.org/10.3390/geosciences9120511

Müller-Navarra S, Bork I (2011) Development of an operational Elbe tidal estuary model. Coast Eng Proc 32:management48. https://doi.org/10.9753/icce.v32.management.48

Moral Ituarte L (1993) El cultivo Del Arroz En Las Marismas Del guadalquivir. Consejería de Agricultura, Junta de Andalucía

Muñoz-López P, García-Lafuente J, Nadal I, Sammartino S (2025) Numerical modeling of the influence of tidal flats on estuaries: the case of the Guadalquivir estuary, SW of the Iberian Peninsula. Front Mar Sci 12:1608858. https://doi.org/10.3389/fmars.2025.1608858

Muñoz-López P, Nadal I, García-Lafuente J, Sammartino S, Bejarano A (2024) Numerical modeling of tidal propagation and frequency responses in the Guadalquivir estuary (SW Iberian Peninsula). Cont Shelf Res 279:105275. https://doi.org/10.1016/j.csr.2024.105275

NOAA CO-OPS (2020) Operational Forecast System. https://tidesandcurrents.noaa.gov/models.html

Ruiz J, Polo MJ, Díez-Minguito M, Navarro G, Morris E, Huertas E, Caballero I, Contreras E, Losada M (2015) The guadalquivir estuary: a hot spot for environmental and human conflicts. In: *Environmental management and governance*. Coastal Res Libr 8:199–232. https://doi.org/10.1007/978-3-319-06305-8_8

Ruiz Pacheco JA, Padorno-Prieto E, Santos-Atienza I, Martínez-Marco I (2018) Verificación Del Modelo HARMONIE-AROME configurado a muy Alta resolución. Acta Jorn Cient AME 35:278. https://doi.org/10.30859/ameJrCn35p278

Savenije HHG (2012) *Salinity and tides in alluvial estuaries*, 2nd completely revised edn. TU Delft, Delft

Siles-Ajamil R, Díez-Minguito M, Losada M (2019) Tide propagation and salinity distribution response to changes in water depth and channel network in the Guadalquivir River estuary: an exploratory model approach. Ocean Coast Manag 174:92–107. https://doi.org/10.1016/j.ocecoaman.2019.03.015

UNESCO-IOC (2020) Quality Control of *in situ* Sea-Level Observations: A Review and Progress towards Automated Quality Control, Vol 1. IOC Manuals and Guides 83, Paris

Wang ZB, Winterwerp JC, He Q (2014) Interaction between suspended sediment and tidal amplification in the Guadalquivir Estuary. Ocean Dynam 64:1487–1498. https://doi.org/10.1007/s10236-014-0758-x